Designing of Anion-Functionalized Ionic Liquids for Efficient Capture of SO_2 from Flue Gas

Kaihong Chen, Wenjun Lin, Xini Yu, Xiaoyan Luo, Fang Ding, Xi He, and Haoran Li
Dept. of Chemistry, ZJU-NHU United R&D Center, Zhejiang University, Hangzhou 310027, People's Republic of China

Congmin Wang
Dept. of Chemistry, ZJU-NHU United R&D Center, Zhejiang University, Hangzhou 310027, People's Republic of China

Key Laboratory of Biomass Chemical Engineering of Ministry of Education, Zhejiang University, Hangzhou 310027, People's Republic of China

DOI 10.1002/aic.14793
Published online March 27, 2015 in Wiley Online Library (wileyonlinelibrary.com)

Five kinds of anion-functionalized ionic liquids (ILs) with different basicity and substituent were selected, prepared and applied in the capture of SO_2 from flue gas, where the concentration of SO_2 is only 2000 ppm. The effect of the anion on SO_2 absorption capacity, desorption residue, and available absorption capacity under 2000 ppm was investigated. The relationship between available absorption capacity and absorption enthalpy was also studied. Through a combination of thermodynamic analysis and quantum calculation, the results indicated that the effect of the cation in the IL on absorption enthalpy was significant. However, the effect of chain length in the cation was weak. Hence, a new IL with low molecular weight, $[P_{4442}][Tetz]$, was further designed and applied for the capture of SO_2, which shows the high absorption capacity of 0.18 g SO_2 per g IL and excellent reversibility for 2000 ppm SO_2. © 2015 American Institute of Chemical Engineers *AIChE J*, 61: 2028–2034, 2015
Keywords: ionic liquids, flue gas desulfurization, thermodynamics analysis, quantum calculation

Introduction

With the increasingly serious air pollution around people, the hot topic about air purification will last for a long time. SO_2, the prime source of atmospheric pollution that hazards the environment and human health, has attracted increased attention. Although the concentration of SO_2 is at a low degree (about 2000 ppm) in flue gas, it will make a great difference in CO_2-capture process, for its irreversible reaction with the absorbent and reducing its capacity. That is why we should eliminate SO_2 ahead of CO_2.[1,2] In industry, the flue gas desulfurization is a kind of classic and effective mode to remove SO_2 from the flue gas. However, these processes also bear plenty of disadvantages, such as the production of wastewater and useless metal salts (e.g., calcium sulfate), where they use limestone or organic solvent as the absorbent.[3–9]

In the past decades, ionic liquids (ILs) have experienced rapid development, because of their unique properties, such as negligible vapor pressure, wide liquid temperature range, tunable structure, and high thermal stability.[10–19] Thanks to these properties, ILs have been proved to be the ideal absorbent for many gases such as SO_2,[20–29] CO_2,[30–38] H_2S,[39–42] CO,[43] and NO_x.[44,45] For instance, Han and coworkers demonstrated the first example of SO_2 chemical absorption by functionalized ILs, tetramethylguanidinium lactate, which absorbed about 1 mol SO_2 per mol IL with 8% SO_2 in a gas mixture of SO_2 and N_2 under ambient pressure.[27] After that, some other functionalized ILs were explored for SO_2 capture, including guanidinium-based ILs,[26,46,47] imidazolium ILs,[2,48–51] and supported ionic liquid membranes.[52–54] Generally, these methods were mainly based on the strong interactions between SO_2 with some nucleophilic atoms[21,55–57] such as O or N atom. Recently, multiple-site absorption was developed as a novel strategy for improving SO_2 capture, where the absorption capacity was up to 4.8 mol SO_2 per mol IL.[24] With the study goes further, a dual-tuning method for both enhancing SO_2 absorption capacity and decreasing absorption enthalpy was developed, which leads to the enhanced absorption capacity and improved desorption simultaneously.[22]

Although SO_2 capture by these functionalized ILs has made significant progresses, little attention was given to SO_2 capture in a very low concentration, such as SO_2 from flue gas (about 2000 ppm). In this respect, a strong chemical interaction with SO_2 is necessary for these ILs, which often means a high absorption enthalpy. However, for the release of SO_2 and the reusability of the ILs, the low absorption enthalpy is desired, since high absorption enthalpy leads to difficult desorption and high energy consumption for desorption. Thus, how to design a functionalized IL with proper absorption enthalpy is critical for the efficient capture of SO_2 in such a low concentration.

Additional Supporting Information may be found in the online version of this article.

Correspondence concerning this article should be addressed to C. Wang at chewcm@zju.edu.cn.

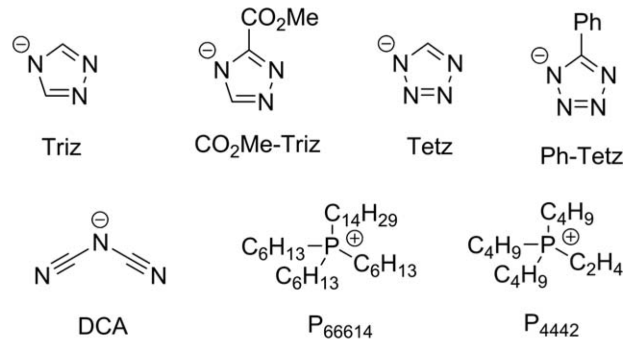

Scheme 1. The structures of the cation and the anion in anion-functionalized ILs for SO_2 capture under 2000 ppm.

In this work, several kinds of anion-functionalized ILs with different basicity and different substituent were selected, prepared, and applied for the capture of SO_2 in a low concentration of 2000 ppm. The effect of the basicity and the substituent of the anion on the SO_2 absorption capacity, desorption residue, and available absorption capacity was investigated under 2000 ppm. Moreover, the relationship between the available absorption capacity and absorption enthalpy was studied. Through a combination of absorption experiment, thermodynamics analysis, and quantum calculation, the results show that the anion [Tetz] is an excellent candidate and the effect of chain length in the cation is weak. Thus, a new IL with low molecular weight, [P_{4442}][Tetz], was further designed and applied for the capture of 2000 ppm SO_2, which exhibited the excellent absorption performance.

Experimental

Materials

All chemicals used in this work were purchased from commercial and used without further purification unless otherwise stated. Methyl-1,2,4-triazole-3- carboxylate (CO_2Me-Triz) and trihexyl(tetradecyl)phosphonium dicyanamide ([P_{66614}][DCA]) were purchased from J&K Scientific. Tetrazole (Tetz) and 5-phenyltetrazole (Ph-Tetz) were purchased from Energy Chemistry Co. Trihexyl(tetradecyl)phosphonium bromide ([P_{66614}][Br]), 1,2,4-triazole (Triz), tributylphosphine (P_{444}), and bromoethane were purchased from Aladdin Ind. Co. N_2 (99.99%), SO_2 (0.2%) which was composed of 0.2% SO_2 and 99.8% N_2, and SO_2 (99.9%) were purchased from Hangzhou Jingong Special Gas Co. ^{1}H NMR and ^{13}C NMR spectra were recorded on a Bruker spectrometer (400 or 500 MHz) in $CDCl_3$ with tetramethylsilane as the standard.

The synthesis of the ILs

[P_{4442}]Br was prepared by the procedure reported by the literature method[23] with a slight modification. A solution of bromoethane (1.20 g, 11 mmol) in MeCN (10 mL) was added dropwise via syringe into a solution of P_{444} (2.02 g, 10 mmol) in MeCN (10 mL) at room temperature. Then, the mixture was heated to 60°C and stirred for 1 day. After being cooled to room temperature, MeCN was distilled off under reduced pressure at 70°C, and the residue was washed with ethyl acetate (3 × 20 mL). The product was dried under high vacuum at 80°C for 1 day to give [P_{4442}]Br as a white solid in a yield of 90%.

These anion-functionalized ILs were prepared by the neutralization of azole and an ethanol solution of [P_{66614}]OH or [P_{4442}]OH, which was prepared from [P_{66614}]Br or [P_{4442}]Br using an anion-exchange resin according to the literature method.[33] In a typical preparation, equimolar tetrazole was added to the [P_{66614}]OH solution in ethanol. The mixture was then stirred at room temperature for 12 h. Subsequently, ethanol and water were distilled off at 70°C under reduced pressure. [P_{66614}][Tetz] obtained was dried in high vacuum for 1 day at 80°C. The structures of these anion-functionalized ILs were confirmed by NMR and IR spectroscopy. No impurities were observed in the NMR spectra. The spectra data of these ILs are given in Supporting Information.

Absorption and desorption of SO_2

In a typical absorption of SO_2 from flue gas, SO_2 at 2000 ppm was bubbled through about 1 g IL in a glass container about 5 mL at a flow rate of about 80 mL min^{-1}. The glass container was partly immersed in an oil bath at 20°C. The amount of SO_2 absorbed was determined at regular intervals by an electronic balance with an accuracy of ±0.0001 g.

The IL was regenerated by bubbling N_2 at 80°C through the IL. In a typical desorption of SO_2, N_2 of atmospheric pressure was bubbled through about 1.0 g IL that captured SO_2 in a glass container, which was partly immersed in a circulated oil bath at 80°C, and the flow rate was about 100 mL min^{-1}. The desorption of SO_2 was determined at regular intervals by an electronic balance with an accuracy of ±0.0001 g.

Calculation method

All calculations were performed using the GAUSSIAN03 programs package. For each set of calculations, we calculated geometry optimization for each free anion, the free SO_2 molecule, and each anion-SO_2 complex at the B3LYP/6–31++G (d,p) level.

Results and Discussion

Absorption of SO_2

In the real situation, we would like to have the IL that can absorb SO_2 as much as it can, and can release SO_2 effectively. In other words, the suitable ILs must have a high available absorption capacity, which is the difference between SO_2 absorption capacity and desorption residue. Especially for the capture SO_2 from flue gas, the strong interaction between the anion in the ILs and SO_2 plays a key role in these processes.[21,22,24,58] Accordingly, three kinds of anions with different basicity were chosen, where the pKa values in DMSO, including [Triz], [Tetz] and [DCA], range from 13.9 to 5.1 (Scheme 1).[59] Furthermore, two kinds of substituted group containing an interaction site such as phenyl group was introduced on the anion to further improve SO_2 absorption (Scheme 1).[20,60]

The SO_2 absorption capacity of these anion-functionalized ILs under 2000 ppm was investigated, which was listed in Table 1. It was seen that the effect of the anion on SO_2 absorption and desorption were significant. Strong basicity led to high SO_2 absorption capacity, however, the desorption residue was high. On the contrary, weak basicity resulted in

Table 1. The SO_2 Absorption by Five Kinds of Anion-Functionalized ILs Under 2000 ppm[a]

Ionic Liquid	Absorption Capacity[b]	Desorption Residue[b]	Available Absorption[c]	pK_a in DMSO	Absorption Enthalpy[d]
$[P_{66614}]$[Triz]	1.22	0.89	0.33	13.9	−107.2
$[P_{66614}]$[CO_2Me-Triz]	0.95	0.26	0.69	–	−93.1
$[P_{66614}]$[Tetz]	0.87	0.06	0.81	8.2	−89.4
$[P_{66614}]$[Ph-Tetz]	0.67	0.00	0.67	–	−72.3
$[P_{66614}]$ [DCA]	0.09	0.00	0.09	5.1	−57.0

[a]The absorption was carried out at 20°C for 5 h, and the desorption was carried out at 80°C for 1 h.
[b]Mol SO_2 per mol IL.
[c]Equal to the absorption capacity minus the desorption residue.
[d]Calculated values between the anion and SO_2 based on B3LYP 6–31++G(d,p) method, kJ/mol.

low desorption residue, while the SO_2 absorption capacity was also low. For example, for the IL $[P_{66614}]$[Triz] with strong basicity, SO_2 absorption capacity and desorption residue were 1.22 and 0.89 mol SO_2 per mol IL, respectively; However, for the IL $[P_{66614}]$[DCA] with weak basicity, the SO_2 absorption capacity and desorption residue were 0.09 and 0 mol SO_2 per mol IL, respectively. Clearly, SO_2 absorption capacity and desorption residue increased with the increase of the basicity of the ILs. Furthermore, the presence of the substituted groups such as phenyl group led to the improved desorption performance, however, SO_2 absorption capacity did not increase because the interaction between the substituted groups and SO_2 was weak.

Table 1 also shows the effect of the anion on SO_2 available absorption capacity. It can be seen that SO_2 available absorption capacity increased from 0.33 to 0.81 mol SO_2 per mol IL when the pKa values of the anion reduced from 13.9 to 8.2. However, when the pKa values of the anion further reduced to 5.1, SO_2 available absorption capacity reduced to 0.09 mol SO_2 per mol IL. Obviously, the IL $[P_{66614}]$[Tetz] with moderate basicity exhibited the best performance under 2000 ppm SO_2.

The relationship between SO_2 absorption performance and absorption enthalpy

To further investigate the relationship between SO_2 absorption performance and the interaction of the ILs with SO_2, quantum chemical calculation was used as a useful tool. Generally, the calculated absorption enthalpy (ΔH_{cal}) between the anion and SO_2 is a key parameter to evaluate the interaction between the IL and SO_2.[24,61,62] Figure 1 shows the relationship between SO_2 absorption capacity under 2000 ppm and ΔH_{cal} between the anion and SO_2 for these anion-functionalized ILs. It was seen that SO_2 absorption capacity reduced with decreasing the ΔH_{cal}. For instance, SO_2 absorption capacity decreased significantly from 1.22 to 0.09 when the ΔH_{cal} reduced from −107.2 to −57.0 kJ/mol. Figure 1 also shows the relationship between desorption residue and ΔH_{cal}. It was understandable that desorption residue decreased with the reduction of the ΔH_{cal}.

Figure 2 shows the relationship between SO_2 available absorption capacity under 2000 ppm and ΔH_{cal} for these anion-functionalized ILs, which is a volcano plot. The highest available absorption capacity of 0.81 mol SO_2 per mol IL was achieved when the ΔH_{cal} is −89.4 kJ/mol. It was emphasized that the relationship between SO_2 available absorption capacity and ΔH_{cal} for different SO_2 concentration is different. For example, under 1 bar SO_2, the highest available absorption capacity of 3.67 mol SO_2 per mol IL was reached when the ΔH_{cal} is −93.1 kJ/mol (Supporting Information Table S1). These results showed that the effect of the interaction enthalpy on SO_2 absorption at different SO_2 concentrations was different, which led to different SO_2 available absorption.

On the basis of DFT calculation at B3LYP 6–31++G(d,p) level, the calculated equilibrium constant K, can be obtained using the Eq. 1

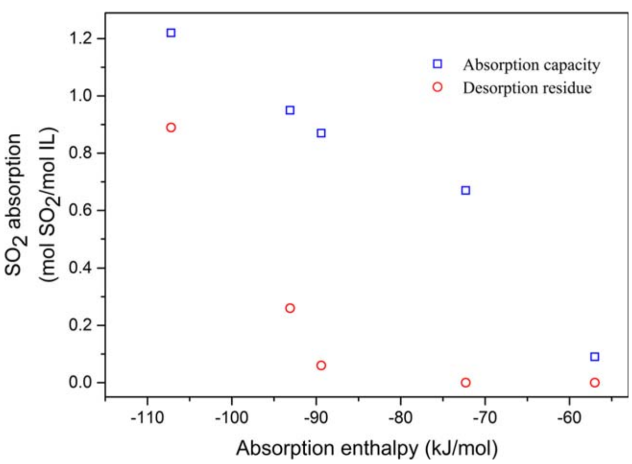

Figure 1. The relationship between absorption capacity or desorption residue and calculated absorption enthalpy ΔH_{cal}.

[Color figure can be viewed in the online issue, which is available at wileyonlinelibrary.com.]

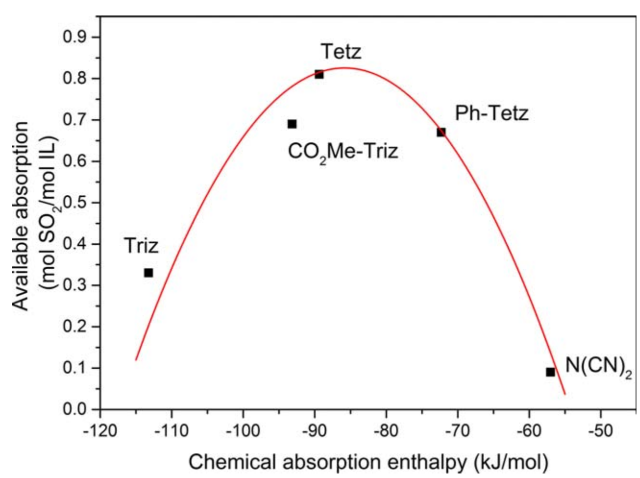

Figure 2. The relationship between available absorption capacity and calculated absorption enthalpy ΔH_{cal}.

[Color figure can be viewed in the online issue, which is available at wileyonlinelibrary.com.]

Table 2. Thermodynamic Constant of Five Kinds of Anion-Functionalized ILs

Ionic Liquid	ΔG^a	K^b
$[P_{66614}]$[Triz]	−68.3	1.48×10^{12}
$[P_{66614}][CO_2Me\text{-}Triz]$	−49.1	5.59×10^{8}
$[P_{66614}]$[Tetz]	−46.7	2.24×10^{8}
$[P_{66614}]$[Ph-Tetz]	−28.8	1.35×10^{5}
$[P_{66614}]$ [DCA]	−12.5	1.70×10^{2}

[a]Calculated values between the anion and SO_2 based on B3LYP 6–31++G(d,p) method, kJ/mol.
[b]Calculated equilibrium constant according to the equation: $\Delta G = -RT\ln(K)$.

$$\Delta G = -RT\ln(K) \tag{1}$$

To our surprise, for $[P_{66614}]$[Tetz], it reached a very large value of 2.24×10^8 (Table 2). In common sense, it can be considered as a completed reaction while the K is beyond 10^5 level. In other words, $[P_{66614}]$[Tetz] should absorb nearly 1 mol SO_2 per mol IL for so large K value. However, according to the experimental results, $[P_{66614}]$[Tetz] can only absorb 0.87 mol SO_2 per mol IL. Why the gap exists between the calculation and experiment result? This puzzle led us to find out a solution.

Thermodynamics analysis

It was known that absorption enthalpy can also be obtained on the basis of the variation of SO_2 absorption capacity with the temperature. Thus, the effect of the temperature on SO_2 absorption by $[P_{66614}]$[Tetz] was investigated (Figure 3). It was seen that SO_2 absorption capacity decreased with the increase of the temperature. For example, SO_2 absorption capacity decreased from 0.87 to 0.07 mol per mol IL when the temperature increased from 20°C to 85°C.

During SO_2 absorption by the IL $[P_{66614}]$[Tetz], physical and chemical absorption are two kinds of SO_2 absorption, which can be easily expressed as Eqs. 2 and 3, respectively

$$SO_2(g) \xrightarrow{H} SO_2(l) \tag{2}$$

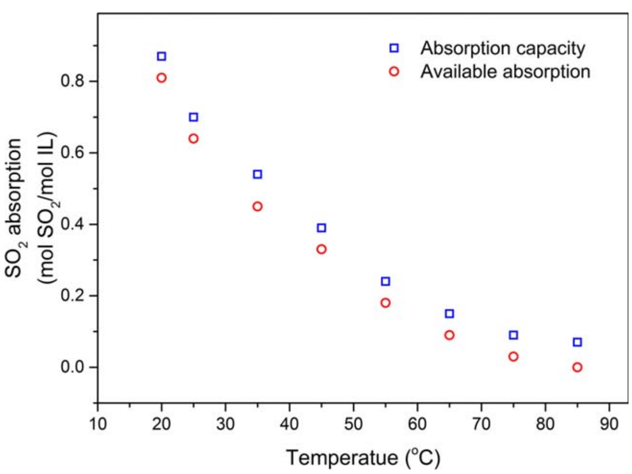

Figure 3. The effect of the temperature on SO_2 absorption under 2000 ppm by $[P_{66614}]$[Tetz].

[Color figure can be viewed in the online issue, which is available at wileyonlinelibrary.com.]

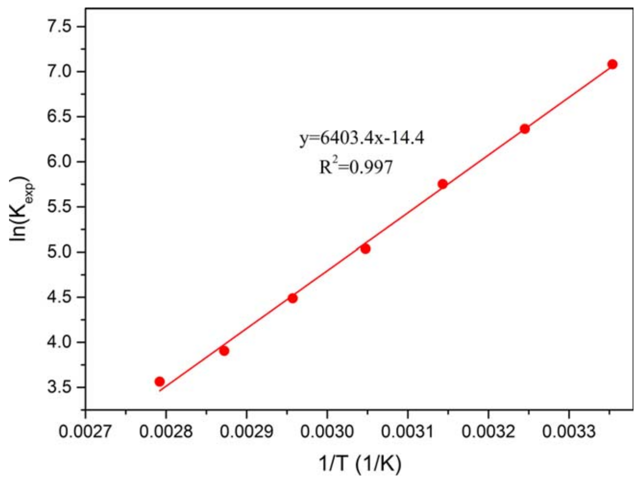

Figure 4. The linear relationship between $\ln(K_{exp})$ and 1/T for $[P_{66614}]$[Tetz].

[Color figure can be viewed in the online issue, which is available at wileyonlinelibrary.com.]

$$SO_2(l) + IL(l) \xrightarrow{K} IL-SO_2(l) \tag{3}$$

where H is Henry's constant and K is equilibrium constant. An overall reaction is showed as

$$SO_2(g) + IL(l) \rightarrow IL-SO_2(l) \tag{4}$$

Considering that physical solubility of SO_2 in $[P_{66614}]$[Tetz] can be ignored because the concentration of SO_2 is very low, a model can be obtained to fit the isotherm data according to the Eq. 5

$$K = \frac{x_{SO_2}}{P_{SO_2}(1 - x_{SO_2})} \tag{5}$$

where the x_{SO_2} is SO_2 absorption capacity on a molar ratio basis. P_{SO2} is the SO_2 pressure in bar.

Thus, SO_2 absorption enthalpy can be obtained from the temperature-dependence of the equilibrium constants K according to the van't Hoff equation, Eq. 6, which is shown in Figure 4. As seen, this plot has a good linear relationship between ln(K) and 1/T, and the value of R^2 is 0.997. The experimental absorption enthalpy ΔH was found to be −53.2 kJ/mol for $[P_{66614}]$[Tetz]

$$\ln(K) = -\frac{\Delta H}{RT} - \frac{\Delta S}{R} \tag{6}$$

However, according to the calculated results, the ΔH_{cal} is −89.4 kJ/mol. There is a big gap of more than 30 kJ/mol between them. What led to the significant difference between them?

Effect of the cation on the calculated absorption enthalpy

Generally, the microenvironment including the anion-cation and ion-solvent interactions of ILs would influence the binding energy of ILs.[62,63] Among them, the cation in the ILs would often influence the gas absorption significantly.[65–69] In this point, it is possible that the gap may be caused by the cation that was not considered during the calculation. In this regard, $[P_{1111}]^+$ was taken into consideration as a model during the calculation at the B3LYP/6-31G++(d,p) level. The optimized structures and the

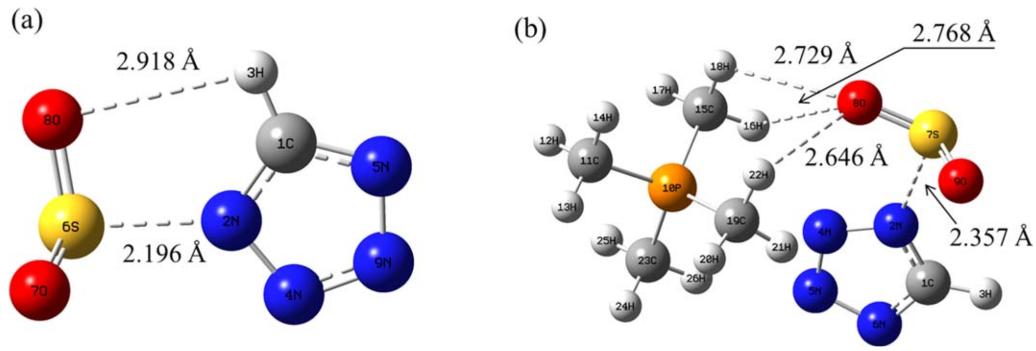

Figure 5. The optimized structures of [Tetz]-SO_2 and [P_{1111}][Tetz]-SO_2 at B3LYP 6–31++G(d,p) level.
[Color figure can be viewed in the online issue, which is available at wileyonlinelibrary.com.]

energetics of [Tetz]-SO_2 and [P_{1111}][Tetz]-SO_2 were showed in Figure 5. It can be seen in Figure 5a that the distance of $S_6 \ldots N_2$ in [Tetz]-SO_2 is predicted to be 2.196 Å, while O_8 and H_3 would have a weak interaction (the distance between them is 2.918 Å). As for [P_{1111}][Tetz]-SO_2, the distance of $S_7 \ldots N_2$ in [P_{1111}][Tetz]-SO_2 is predicted to be 2.357 Å, which is further than that in [Tetz]-SO_2. In addition, O_9 and H_3 would have no interaction anymore, for such a far distance (3.792 Å, Figure 5b). All of these clues indicate that the interaction between [Tetz] and SO_2 is weaker when $[P_{1111}]^+$ is introduced in the calculation. Furthermore, the calculated absorption enthalpy ΔH_{cal} is −63.6 kJ/mol when regarding [P_{1111}] as the cation, which is significantly lower than that of −89.4 kJ/mol for [Tetz]-SO_2, also indicating the weaker interaction for [P_{1111}][Tetz]. These results demonstrate that the effect of the cation on SO_2 absorption enthalpy during the calculation is significant, leading to the big gap between them.

The effect of the length of the alkyl chains in the cation on the calculated absorption enthalpy was also investigated, which was shown in Table 3. It was seen that the effect of the chain length in the cation on absorption enthalpy was weak. For example, absorption enthalpies for [P_{1112}][Tetz] and [P_{2222}][Tetz] were −63.5 and −61.8 kJ/mol, respectively. Clearly, the calculated absorption enthalpy is closer to the experimental value when the cation was considered during the calculation.

Table 3. The Effect of Chain Length in the Cation on Calculated SO_2 Absorption Enthalpy[a]

	[Tetz]	[P_{1111}][Tetz]	[P_{1112}][Tetz]	[P_{2222}][Tetz]
ΔH_{cal}	−89.4	−63.6	−63.5	−61.8

[a]Based on B3LYP6-31++G(d,p) method, kJ/mol.

Table 4. The SO_2 Absorption by [P_{4442}][Tetz] Under 2000 ppm

Ionic liquid	Absorption Capacity[a]	Desorption Residue[a]	Available Absorption[b]
[P_{4442}][Tetz][c]	0.90	0.07	0.83

[a]Mol SO_2 per mol IL.
[b]Equal to the absorption capacity minus the desorption residue.
[c]The absorption was carried out at 20°C for 9 h, and the desorption was carried out at 80°C for 1 h.

The design of [P_{4442}][Tetz] and its reusability

For the real situation, SO_2 absorption capacity based on the weight is more important. Furthermore, according to the above calculated results, the effect of the length of the alkyl chains in the cation on absorption enthalpy was weak. Therefore, a new IL with low molecular weight, [P_{4442}][Tetz], was designed, prepared and used for SO_2 absorption under 2000 ppm, which was shown in Table 4. It was seen that [P_{4442}][Tetz] captured 0.90 mol SO_2 per mol IL at 20°C under 2000 ppm SO_2, and the desorption residue was 0.07 mol SO_2 per mol IL at 80°C for 1 h, which was similar with that by [P_{66614}][Tetz]. The effect of water on SO_2 capture was also investigated, which was shown in Supporting Information Table S2. As can be seen, the effect of water on the absorption of SO_2 by [P_{4442}][Tetz] was weak. To the best of our knowledge, compared with dozens of ILs for the capture of SO_2, [P_{4442}][Tetz] exhibits the highest available absorption capacity under 2000 ppm SO_2, where the available absorption capacity is 0.18 g SO_2 per g IL (Table 5).

Table 5. The Comparison of SO_2 Available Absorption at Low Concentration by [P_{4442}][Tetz] with Other ILs

Ionic Liquids[a]	SO_2 Concentration	Absorption Temperature/°C	Available Absorption[b]	Reference
[P_{4442}][Tetz]	2000 ppm	20	0.18	This work
[P_{66614}][BenIm]	2000 ppm	20	0.06	20
[C_{10}mim][Tetz]	2000 ppm	20	0.13	23
[N_{2224}][disuccinate]	4000 ppm	40	0.12	28
[N_{2222}][diglutarate]	2000 ppm	40	0.12	29
[DMEA][diglutarate]	4000 ppm	40	0.11	29
[MEA]L	3440 ppm	25	0.11	67
[TMG]L	3440 ppm	25	0.16	67

[a][C_{10}mim][Tetz], 1-decyl-3-methyl imidazolium tetrazole; [P_{66614}][BenIm], trihexyl(tetradecyl)phosphonium benzimidazolate; [TMG]L, 1,1,3,3-tetramethylguanidinium lactate; [MEA]L, monoethanolaminium lactate; [N_{2222}][diglutarate], tetraethylammonium diglutarate; [DMEA][diglutarate], dimethylethanolammonium diglutarate; [N_{2224}][disuccinate], triethylbutylammonium disuccinate.
[b]Absorption capacity on the basis of weight, g SO_2 per g IL.

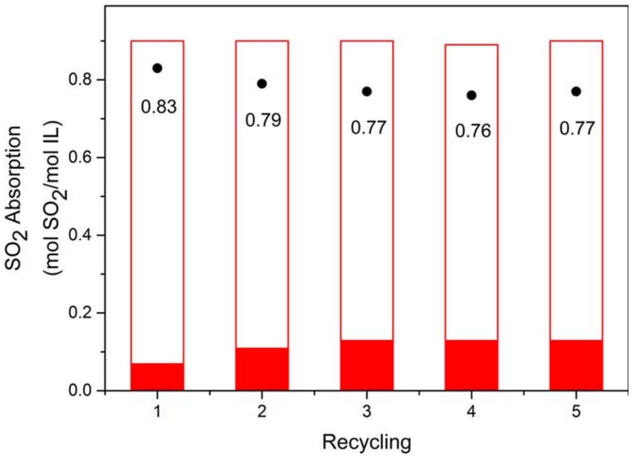

Figure 6. SO_2 absorption by [P_{4442}][Tetz] for 5 cycles.

[Color figure can be viewed in the online issue, which is available at wileyonlinelibrary.com.]

The reusability of an IL is a critical property for gas absorption, which has a direct impact on the costs because it determines the frequency of the IL's replacement. Therefore, we selected [P_{4442}][Tetz] as a sorbent material to investigate the stability of SO_2 absorption under 2000 ppm during the recycling of the IL. The results for 5 absorption/desorption cycles of [P_{4442}][Tetz] were shown in Figure 6. To our delight, the high available absorption capacity was well-maintained during the 5 cycles, which indicates that the SO_2 absorption process by [P_{4442}][Tetz] is highly reversible.

Conclusion

In conclusion, the effect of the basicity and substituent in the anion on SO_2 absorption under 2000 ppm was investigated, indicating that the effect of the basicity and substituent on absorption capacity, desorption residue, and available absorption capacity was significant. The relationship between available absorption capacity and absorption enthalpy was investigated, which is a volcano plot. Through a combination of thermodynamic analysis and quantum calculation, the results demonstrated the importance of the cation in the calculation as well as the weak effect of chain length in the cation. Therefore, a new designed IL with low molecular weight, [P_{4442}][Tetz], was applied to SO_2 capture under 2000 ppm, which exhibits the high SO_2 available absorption capacity of 0.18 g SO_2 per g IL and excellent reversibility. We believe this method can be used in other gases capture and be helpful for designing the effective absorbent.

Acknowledgments

This work was supported by the National Key Basic Research Program of China (2015CB251401), the National Natural Science Foundation of China (21176205, 21322602, J1210042), the Zhejiang Provincial Natural Science Foundation of China (R12BL06002), the Program for Zhejiang Leading Team of S&T Innovation (2011R50007), and the Fundamental Research Funds of the Central Universities for financial support.

Literature Cited

1. Rao AB, Rubin ES. A technical, economic, and environmental assessment of amine-based CO_2 capture technology for power plant greenhouse gas control. *Environ Sci Technol*. 2002;36:4467–4475.
2. Anderson JL, Dixon JK, Maginn EJ, Brennecke JF. Measurement of SO_2 solubility in ionic liquids. *J Phys Chem B*. 2006;110:15059–15062.
3. Zheng YJ, Kiil S, Johnsson JE. Experimental investigation of a pilot-scale jet bubbling reactor for wet flue gas desulphurisation. *Chem Eng Sci*. 2003;58:4695–4703.
4. Kikkawa H, Nakamoto T, Morishita M, Yamada K. New wet FGD process using granular limestone. *Ind Eng Chem Res*. 2002;41:3028–3036.
5. Ma XX, Kaneko T, Tashimo T, Yoshida T, Kato K. Use of limestone for SO_2 removal from flue gas in the semidry FGD process with a powder-particle spouted bed. *Chem Eng Sci*. 2000;55:4643–4652.
6. Han DH, Sohn HY. Calcined calcium magnesium acetate as a superior SO_2 sorbent: I. Thermal decomposition. *AIChE J*. 2002;48:2971–2977.
7. Sohn HY, Han DH. Ca-Mg acetate as dry SO_2 sorbent: II. Sulfation of CaO in calcination product. *AIChE J*. 2002;48:2978–2984.
8. Sohn HY, Han DH. Ca-Mg acetate as dry SO_2 sorbent: III. Sulfation of MgO+CaO. *AIChE J*. 2002;48:2985–2991.
9. Bausach M, Pera-Titus M, Fite C, Cunill F, Izquierdo JF, Tejero J, Iborra M. Kinetic modeling of the reaction between hydrated lime and SO_2 at low temperature. *AIChE J*. 2005;51:1455–1466.
10. Hallett JP, Welton T. Room-temperature ionic liquids: solvents for synthesis and catalysis. *2. Chem Rev*. 2011;111:3508–3576.
11. Blanchard LA, Hancu D, Beckman EJ, Brennecke JF. Green processing using ionic liquids and CO_2. *Nature*. 1999;399:28–29.
12. Welton T. Room-temperature ionic liquids. solvents for synthesis and catalysis. *Chem Rev*. 1999;99:2071–2084.
13. Brennecke JF, Maginn EJ. Ionic liquids: innovative fluids for chemical processing. *AIChE J*. 2001;47:2384–2389.
14. Greaves TL, Drummond CJ. Protic ionic liquids: properties and applications. *Chem Rev*. 2008;108:206–237.
15. Wasserscheid P, Keim W. Ionic liquids—new "solutions" for transition metal catalysis. *Angew Chem Int Ed*. 2000;39:3772–3789.
16. Huang JF, Luo HM, Liang CD, Sun IW, Baker GA, Dai S. Hydrophobic bronsted acid-base ionic liquids based on PAMAM dendrimers with high proton conductivity and blue photoluminescence. *J Am Chem Soc*. 2005;127:12784–12785.
17. Bara JE, Gabriel CJ, Hatakeyama ES, Carlisle TK, Lessmann S, Noble RD, Gin DL. Improving CO_2 selectivity in polymerized room-temperature ionic liquid gas separation membranes through incorporation of polar substituents. *J Membr Sci*. 2008;321:3–7.
18. Soutullo MD, Odom CI, Wicker BF, Henderson CN, Stenson AC, Davis JH, Jr. Reversible CO_2 capture by unexpected plastic-, resin-, and gel-like ionic soft materials discovered during the combi-click generation of a TSIL library. *Chem Mater*. 2007;19:3581–3583.
19. Anderson JL, Ding RF, Ellern A, Armstrong DW. Structure and properties of high stability geminal dicationic ionic liquids. *J Am Chem Soc*. 2005;127:593–604.
20. Cui GK, Lin WJ, Ding F, Luo XY, He X, Li HR, Wang CM. Highly efficient SO_2 capture by phenyl-containing azole-based ionic liquids through multiple-site interactions. *Green Chem*. 2014;16:1211–1216.
21. Wang CM, Zheng JJ, Cui GK, Luo XY, Guo Y, Li HR. Highly efficient SO_2 capture through tuning the interaction between anion-functionalized ionic liquids and SO_2. *Chem Commun*. 2013;49:1166–1168.
22. Cui GK, Zheng JJ, Luo XY, Lin WJ, Ding F, Li HR, Wang CM. Tuning anion-functionalized ionic liquids for improved SO_2 capture. *Angew Chem Int Ed*. 2013;52:10620–10624.
23. Cui GK, Wang CM, Zheng JJ, Guo Y, Luo XY, Li HR. Highly efficient SO_2 capture by dual functionalized ionic liquids through a combination of chemical and physical absorption. *Chem Commun*. 2012;48:2633–2635.
24. Wang CM, Cui GK, Luo XY, Xu YJ, Li HR, Dai S. Highly efficient and reversible SO_2 capture by tunable azole-based ionic liquids through multiple-site chemical absorption. *J Am Chem Soc*. 2011;133:11916–11919.
25. Ren SH, Hou YC, Wu WZ, Liu QY, Xiao YF, Chen XT. Properties of ionic liquids absorbing SO_2 and the mechanism of the absorption. *J Phys Chem B*. 2010;114:2175–2179.
26. Huang J, Riisager A, Wasserscheid P, Fehrmann R. Reversible physical absorption of SO_2 by ionic liquids. *Chem Commun*. 2006;38:4027–4029. .
27. Wu WZ, Han BX, Gao HX, Liu ZM, Jiang T, Huang J. Desulfurization of flue gas: SO_2 absorption by an ionic liquid. *Angew Chem Int Ed*. 2004;43:2415–2417.

28. Huang K, Wang GN, Dai Y, Wu YT, Hu XB, Zhang ZB. Dicarboxylic acid salts as task-specific ionic liquids for reversible absorption of SO_2 with a low enthalpy change. *RSC Adv.* 2013;3:16264–16269.
29. Huang K, Chen YL, Zhang XM, Xia S, Wu YT, Hu XB. SO_2 absorption in acid salt ionic liquids/sulfolane binary mixtures: experimental study and thermodynamic analysis. *Chem Eng J*. 2014;237: 478–486.
30. Wang CM, Luo HM, Jiang DE, Li HR, Dai S. Carbon dioxide capture by superbase-derived protic ionic liquids. *Angew Chem Int Ed.* 2010;49:5978–5981.
31. Wang CM, Luo HM, Luo XY, Li HR, Dai S. Equimolar CO_2 capture by imidazolium-based ionic liquids and superbase systems. *Green Chem.* 2010;12:2019–2023.
32. Wang CM, Mahurin SM, Luo HM, Baker GA, Li HR, Dai S. Reversible and robust CO_2 capture by equimolar task-specific ionic liquid–superbase mixtures. *Green Chem.* 2010;12:870–874.
33. Wang CM, Luo XY, Luo HM, Jiang DE, Li HR, Dai S. Tuning the basicity of ionic liquids for equimolar CO_2 capture. *Angew Chem Int Ed*. 2011;50:4918–4922.
34. Wang CM, Guo Y, Zhu X, Cui GK, Li HR, Dai S. Highly efficient CO_2 capture by tunable alkanolamine-based ionic liquids with multidentate cation coordination. *Chem Commun.* 2012;48:6526–6528.
35. Wang CM, Luo HM, Li HR, Zhu X, Yu B, Dai S. Tuning the physicochemical properties of diverse phenolic ionic liquids for equimolar CO_2 capture by the substituent on the anion. *Chem Eur J*. 2012;18: 2153–2160.
36. Bates ED, Mayton RD, Ntai I, Davis JH. CO_2 capture by a task-specific ionic liquid. *J Am Chem Soc*. 2002;124:926–927.
37. Zhang YQ, Zhang SJ, Lu XM, Zhou Q, Fan W, Zhang XP. Dual amino-functionalised phosphonium ionic liquids for CO_2 capture. *Chem Eur J*. 2009;15:3003–3011.
38. Bara JE, Camper DE, Gin DL, Noble RD. Room-temperature ionic liquids and composite materials: platform technologies for CO_2 capture. *Acc Chem Res*. 2010;43:152–159.
39. Jou FY, Mather AE. Solubility of hydrogen sulfide in bmim PF_6. *Int J Thermophys*. 2007;28:490–495.
40. Jalili AH, Rahmati-Rostami M, Ghotbi C, Hosseini-Jenab M, Ahmadi AN. Solubility of H_2S in ionic liquids bmim PF_6, bmim BF_4, and bmim Tf_2N. *J Chem Eng Data*. 2009;54:1844–1849.
41. Shiflett MB, Niehaus AMS, Yokozeki A. Separation of CO_2 and H_2S using room-temperature ionic liquid bmim $MeSO_4$. *J Chem Eng Data*. 2010;55:4785–4793.
42. Huang K, Cai DN, Chen YL, Wu YT, Hu XB, Zhang ZB. Thermodynamic validation of 1-alkyl-3-methylimidazolium carboxylates as task-specific ionic liquids for H_2S absorption. *AIChE J*. 2013;59: 2227–2235.
43. Raeissi S, Florusse LJ, Peters CJ. Purification of flue gas by ionic liquids: carbon monoxide capture in [bmim][Tf_2N]. *AIChE J*. 2013; 59:3886–3891.
44. Revelli AL, Mutelet F, Jaubert JN. Reducing of nitrous oxide emissions using ionic liquids. *J Phys Chem B*. 2010;114:8199–8206.
45. Shiflett MB, Niehaus AMS, Yokozeki A. Separation of N_2O and CO_2 using room-temperature ionic liquid bmim BF_4. *J Phys Chem B*. 2011;115:3478–3487.
46. Huang J, Riisager A, Berg RW, Fehrmann R. Tuning ionic liquids for high gas solubility and reversible gas sorption. *J Mol Catal A: Chem.* 2008;279:170–176.
47. Wang Y, Pan H, Li HR, Wang CM. Force field of the TMGL ionic liquid and the solubility of SO_2 and CO_2 in the TMGL from molecular dynamics simulation. *J Phys Chem B*. 2007;111:10461–10467.
48. Yokozeki A, Shiflett MB. Separation of carbon dioxide and sulfur dioxide gases using room-temperature ionic liquid hmim Tf_2N. *Energy Fuels.* 2009;23:4701–4708.
49. Shiflett MB, Yokozeki A. Chemical absorption of sulfur dioxide in room-temperature ionic liquids. *Ind Eng Chem Res.* 2010;49:1370–1377.
50. Shiflett MB, Yokozeki A. Separation of carbon dioxide and sulfur dioxide using room-temperature ionic liquid bmim $MeSO_4$. *Energy Fuels*. 2010;24:1001–1008.
51. Yang DZ, Hou MQ, Ning H, Ma J, Kang XC, Zhang JL, Han BX. Reversible capture of SO_2 through functionalized ionic liquids. *ChemSuschem.* 2013;6:1191–1195.
52. Jiang YY, Zhou Z, Jiao Z, Li L, Wu YT, Zhang ZB. SO_2 gas separation using supported ionic liquid membranes. *J Phys Chem B*. 2007;111:5058–5061.
53. Luis P, Neves LA, Afonso CAM, Coelhoso IM, Crespo JG, Garea A, Irabien A. Facilitated transport of CO_2 and SO_2 through supported ionic liquid membranes (SILMs). *Desalination.* 2009;245: 485–493.
54. Hu XB, Li YX, Huang K, Ma SL, Yu H, Wu YT, Zhang ZB. Impact of alpha-D-glucose pentaacetate on the selective separation of CO_2 and SO_2 in supported ionic liquid membranes. *Green Chem.* 2012; 14:1440–1446.
55. Yang ZZ, He LN, Song QW, Chen KH, Liu AH, Liu XM. Highly efficient SO_2 absorption/activation and subsequent utilization by polyethylene glycol-functionalized Lewis basic ionic liquids. *Phys Chem Chem Phys.* 2012;14:15832–15839.
56. Lee KY, Kim HS, Kim CS, Jung KD. Behaviors of SO_2 absorption in [BMIm][OAc] as an absorbent to recover SO_2 in thermochemical processes to produce hydrogen. *Int J Hydrogen Energy*. 2010;35: 10173–10178.
57. Hong SY, Im J, Palgunadi J, Lee SD, Lee JS, Kim HS, Cheong M, Jung KD. Ether-functionalized ionic liquids as highly efficient SO_2 absorbents. *Energy Environ Sci*. 2011;4:1802–1806.
58. Mohammadi M, Foroutan M. Molecular investigation of SO_2 gas absorption by ionic liquids: effects of anion type. *J Mol Liq*. 2014; 193:60–68.
59. Bordwell, FG. Equilibrium acidities in dimethyl sulfoxide solution. *Acc Chem Res*. 1988;21:456–463.
60. Ding F, He X, Luo XY, Lin WJ, Chen KH, Li HR, Wang CM. Highly efficient CO_2 capture by carbonyl-containing ionic liquids through Lewis acid-base and cooperative C-H…O hydrogen bonding interaction strengthened by the anion. *Chem Commun.* 2014;50: 15041–15044.
61. Wang CM, Luo XY, Luo HM, Jiang DE, Li HR, Dai S. Tuning the basicity of ionic liquids for equimolar CO_2 capture. *Angew Chem Int Ed*. 2011;50:4918–4922.
62. Teague CM, Dai S, Jiang DE. Computational investigation of reactive to nonreactive capture of carbon dioxide by oxygen-containing lewis bases. *J Phys Chem A*. 2010;114:11761–11767.
63. Hu XB, Lin QX, Gao JY, Wu YT, Zhang ZB. Anion–cation and ion–solvent interaction of some typical ionic liquids in solvents with different dielectric constant. *Chem Phys Lett*. 2011;516:35–39.
64. Wakai C, Oleinikova A, Ott M, Weingaitner H. How polar are ionic liquids? determination of the static dielectric constant of an imidazolium-based ionic liquid by microwave dielectric spectroscopy. *J Phys Chem B*. 2005;109:17028–17030.
65. Ren J, Wu LB, Li BG. Potential for using simple 1,2,4-triazole salt solutions as highly efficient CO_2 absorbents with low reaction enthalpies. *Ind Eng Chem Res*. 2013;52:8565–8570.
66. Tian SD, Hou YC, Wu WZ, Ren SH, Zhang C. Absorption of SO_2 by thermal-stable functional ionic liquids with lactate anion. *RSC Adv*. 2013;3:3572.
67. Zeng SJ, Gao HS, Zhang XC, Dong HF, Zhang XP, Zhang SJ. Efficient and reversible capture of SO_2 by pyridinium-based ionic liquids. *Chem Eng J*. 2014;251:248–256.
68. Jin MJ, Hou YC, Wu WZ, Ren SH, Tian SD, Xiao L, Lei ZG. Solubilities and thermodynamic properties of SO_2 in ionic liquids. *J Phys Chem B*. 2011;115:6585–6591.
69. Anderson JL, Dixon JK, Brennecke JF. Solubility of CO_2, CH_4, C_2H_6, C_2H_4, O_2, and N_2 in 1-hexyl-3-methylpyridinium bis(trifluoromethylsulfonyl)imide: comparison to other ionic liquids. *Acc Chem Res*. 2007;40:1208–1216.

Manuscript received Dec. 25, 2014, and revision received Feb. 23, 2015.